SYNTHESIS AND CHARACTERIZATION OF LOW DENSITY STEEL

A DISSERTATION

Submitted in partial fulfilment of the

requirements for the award of the degree

of

MASTER OF TECHNOLOGY

in

METALLURGICAL AND MATERIALS ENGINEERING

by

ATUL CHAUDHRY

DEPARTMENT OF METALLURGICAL AND MATERIALS ENGINEERING

INDIAN INSTITUTE OF TECHNOLOGY ROORKEE

ROORKEE – 247667, INDIA

MAY, 2016

INDIAN INSTITUTE OF TECHNOLOGY ROORKEE

CANDIDATE'S DECLARATION

I hereby certify that the work which is being presented in the thesis, entitled **"SYNTHESIS AND CHARACTERIZATION OF LOW DENSITY STEEL"** has submitted by "**Mr. ATUL CHAUDHRY**" in partial fulfilment of the requirements for the degree of **Master of Technology** in the **Department of Metallurgical and Materials Engineering with specialization in "Physical Metallurgy"**, Indian Institute of Technology Roorkee, is an authentic record of my own work carried out during the period from May, 2015 to April, 2016 under the supervision of **Dr. Sadhan Ghosh**, **Assistant Professor,** Department of Metallurgical and Materials Engineering, Indian Institute of Technology Roorkee, Roorkee.

The matter embodied in the thesis has not been submitted to any of the University/Institute for the award of any other degree.

(**ATUL CHAUDHRY**)

CERTIFICATE

This is to certify that the above statement made by the candidate is correct to the best of our knowledge.

Date: (Dr. Sadhan Ghosh)

Place: Supervisor

ACKNOWLEDGEMENT

First and foremost, all praise is to God.

I would like to express my sincere and deep gratitude to my guide, Dr. Sadhan Ghosh, Assistant professor at Department of Metallurgical and Materials Engineering, Indian Institute of Technology Roorkee, for their encouragement, suggestions, and continuous support during my M.Tech. Study at IIT Roorkee. I would like to thank my professor for giving the opportunity to work on my Master thesis. I am so fortunate to work under your supervision for my project and immensely grateful to all the effort taken by my professor throughout my project.

I am extremely thankful to Dr. Anjan Sil, Professor and Head of the department of Metallurgical and Materials Engineering, Indian Institute of Technology Roorkee, for his help to carry out this dissertation.

I also wish to express my appreciation to Mr. Satish Jaiswal, Mr. Mrinmoy Sinha, Mr. Niranjan Kumar, Mr. Ajay Singh Tomar and Mr. Abhishek Gupta for reviewing my work and serving on my committee.

I cannot forget to thank all my group members especially Mr. Mukul Srivastava and Mr. Nikhil Mohandas for their help and support during my work. I will always remember the laughter and good times we had together.

Special thanks is given to my family for their love, continuous support, understanding and constant encouragement.

ABSTRACT

Steel is an ever green structural material; but, it has a problem of low strength to specific weight ratio. This makes the use of steel in automobile industry slightly a less competitive, due to heavy weight and hence more energy consumption, leading to environmental pollution. In order to reduce density of steels, Al-addition by and large has drawn a large interest. However, it affects the mechanical properties of steel because of formation of hard and brittle intermetallic, namely k carbide. The thermodynamics of Mn addition may be an alternative proposal in the present work, as Fe-Al-Mn-C has the potential to provide exciting mechanical behavior. Melting or Sintering can be used as synthesizing technique for low density steel. Melting causes grain growth, dendritic microstructure and finally segregation of Mn as the allying addition. Thus an alternative route is testified here i.e. non-equilibrium synthesis of low density Fe-C-Mn-Al alloy, aiming for an exotic microstructure. With the advancement of modern technique like spark plasma sintering (SPS), the synthesis of bulk material from the mechanically alloyed powder may be a reality. In to execute this, elemental Fe, C, Mn and Al in desired quantiles were ball milled up to 40 h to ensure the formation of homogeneous solid solution. Thereafter consolidation of fine particle in SPS required optimization of the process parameters through trial and error, as an extensive part of the present research work, recording a temperature of 1000°C, pressure of 60 MPa and 50°C/min heating rate good enough to provide a density of 98.7% by Archimedes principle. Characterization by X-Ray diffraction, optical and scanning electron microscopy were performed to evaluate the microstructure formation, apart from determining equilibrium phase diagram by Thermo-Calc software. The bottom line provides a hardness of 920VHN for SPS sample, as compared to 560VHN for vacuum arc melted sample. The compression test in engineering stress-strain plot provided UTS of 1709 MPa while maintaining an extraordinary high elongation.

TABLE OF CONTENTS

LIST OF FIGURES

LIST OF TABLES

LIST OF ABBREVIATIONS

LDS	Low density steel
DP	Duplex steel
TRIP	Triplex steels
TWIP	Twining induced plasticity
VAM	Vacuum arc melting
VIM	Vacuum induction melting
MA	Mechanical alloying
SPS	Spark plasma sintering
DR	Dynamic recrystallization
Fig.	FIGURE
SEM	Scanning electron microscope
TMP	Thermo-mechanical processing
UTS	Ultimate tensile strength

CHAPTER 1 INTRODUCTION

Steels have established itself as vital component of almost all major manufacturing industries such as automobile, etc. The various other materials have been developed like titanium, chromium alloys which have superior properties than that of steel but these materials are still not as prevalent as steel because steel's material and processing is cost effective and give reasonable strength. Steels main drawback is its low strength to weight ratio which limits its use in light weight applications. In order to remain competitive with other advanced materials its density should be reduced without comprising on strength. Density of steel can be reduced by adding light-weight materials like aluminium, magnesium, silicon, etc.

Energy consumption and pollution are area of concerned of automobile industry due to high weight of materials used in manufacturing parts of automobile. Reduction in density of steels of order of 10% can increase its competitiveness many fold in automobile industry. Fuel efficiency of automobile maximizes with reduction of body parts which can be achieved by using low density steels. Various alloying elements are added in steel to reduce its density without significantly degrading mechanical properties rather enhancing mechanical properties. Evolution of low density steel is dated back to 1933 led to development of Fe-Mn-Al-C system [1]. Many efforts have been made to replace Ni and Cr with Fe and Al. In recent times, research on LDS have again gain attention particularly for automobile industry after a gap of long time. Still a lot of research work is required for making LDS a valuable input for automobile industry. Low density steel has diversity in constituent phases that is it contains ferrite, austenite and kappa carbide phase. This diversity makes LDS a versatile materials for application in automobile industry. Different structural parts of automobile requires varying strength and ductility. This varying strength and ductility can be easily achieved by microstructural modulation of low density steel. For e.g., Ferritic Fe-Al LDS alloy is suitable for closures of automobile where strength required is moderate. The strain hardenability of low density steels is high and have excellent strength as well as ductility. The combination of superior strength of low density steel is because of solid solution effect provided by alloying elements and precipitation hardening due to formation of nano-sized kappa carbide which is coherent to austenite matrix.

Alloying elements for constituting LDS

There are various alloying elements which are added to reduce density of steel as well as to obtain desired microstructure and mechanical properties. Alloying elements plays important role in deciding the properties of steel. Various alloying elements and their effect on steel is described below:

1.1.1 Effect of aluminium addition to steel:

Aluminium is excellent alloying element in order to reduce density of steel because of its light weight. Aluminium addition in steel in range of 6% or more results in considerable reduction in steel's density. Large addition of aluminium has deteriorating effect on steel as it forms intermetallic compound like FeAl, Fe_3Al and k-carbide. These intermetallic compounds reduces the ductility and toughness of steel. The machinability of steel also deteriorates significantly.

1.1.2 Effect of manganese addition to steel:

Manganese is austenite stabilizer and contributes to formation of austenite at higher temperature. Manganese also increase steel's lattice constant thus reduces density of steel. Manganese addition in range of 2.5 to 30 wt. % have been studied. High manganese added steel exhibit austenitic phase and ultra-high strength. However, if the amount of manganese addition in steel is quite large then central segregation can occur which results in formation of band structure in hot rolled sheet which ultimately decreases ductility.

1.1.3 Effect of Carbon addition

Carbon is an austenite stabilizer and provides dispersion hardening by forming precipitates. Carbon involves in creation of cementite $(FeMn)_3C$ and k-carbide $(Fe,Mn)_3AlC$. Carbon between 0.15 to 0.25 wt. % is added to give strength to steel. If carbon is added more than 0.25 wt. % then it increases the strength but significantly reduces the ductility of steel because of formation of excessive carbides particularly k-carbide which forms at grain boundaries of ferrite and give brittleness to steel.

1.1.4 Effect of Nickel

Nickel is an austenite-former and may introduces partial austenite during hot rolling. This will refine structure and results in improving the ridging resistibility. The only limitation is price of steel which is quite high and thus increases cost of manufacturing. That's why its use is limited to 0.1 to 2.0%.

Classification of LDS

Presence of different phases in LDS led to classification of LDS such as ferritic (α) [2,3] austenitic (γ) [4,5] duplex phase (α + γ) [6,7] and triplex phase (α + γ + k- carbides) steels. According to the operative strengthening and ductility-enhancing mechanisms, low-density steels' further classification is done into following categories. High Al-enriched ferritic steels can be interstitial free (IF) [8] and bake hardenable [9]. There are some of the low-density steels containing austenite are precipitation harden able (by k-carbides) [10]. Others could involve transformation-induced plasticity (TRIP; including d-TRIP) [11] twinning-induced plasticity (TWIP) [12] shear band induced plasticity (SIP) [13] or micro band induced plasticity (MBIP) [14] whose classification depends on composition of alloy and process parameters.

1.1.5 Steels classification on basis of presence of phase

Ferritic low density steels

The ferritic (Fe-Al) steels contains ferritic phase at room temperature because of presence of aluminium which is ferrite stabilizer. These type of steels have limitation in strength and ductility and are brittle in nature. Ferritic steels have limitations in formability which restricts its application in automobile industry. It has found that carbon content in Al-containing ferritic steels should be minimized to avoid the possible formation of ordered carbides, $Fe_{4-y}Al_yC_x$ ($0.8 < y < 1.2$; $0 < x < 1$) [15] which are detrimental to sheet formability.

Austenitic low density steels

Austenitic LDS have high manganese (>25wt. %) content and belongs to Fe-Al-Mn-C alloys. These steels are concentrated solid solutions of austenite with an atomic fraction of Fe often less than 0.5. These steels have short range order because of thermodynamic constraint caused by heavy alloying. These short range order still exist even cooling with high rate as in water quenching. Precipitation of k-carbide takes place on existing short range order. Deformation characteristics of austenitic steels is modified by presence of k-carbides and stacking fault energy.

Duplex Steels

Duplex steels are based on Fe-Al-Mn-C system having ferrite and austenite phases. Aluminium is ferrite stabilizer which gives ferritic steels. Austenite stabilizers, carbon and manganese are added to get austenite phase and this is basis of forming duplex steel. The major phase microstructure is decided by relative amounts of depending on the relative amounts of Al and

(Mn + C). If aluminium is high then ferrite can be major phase and if (Mn + C) is high then austenite will be major phase in microstructure [16].The ferrite-based duplex steels are more effective in density reduction than the austenite-based ones because ferritic steels contains more aluminium than austenitic steels.

Triplex low density steel

Triplex steel are based on Fe-Al-Mn-C system and contains Ferrite, Austenite and k-carbide as phases [13] The producing route of triplex steel is same as duplex steels with addition of one extra step which is solution annealing and then quenching. This is followed by aging step in which k-carbide growth takes place in those regions where carbon is in abundance. The growth of K-carbide takes place from carbon enriched areas as shown in Fig.1. Austenite existence occurs from ferrite and then k-carbide forms at interphase of austenite and ferrite.

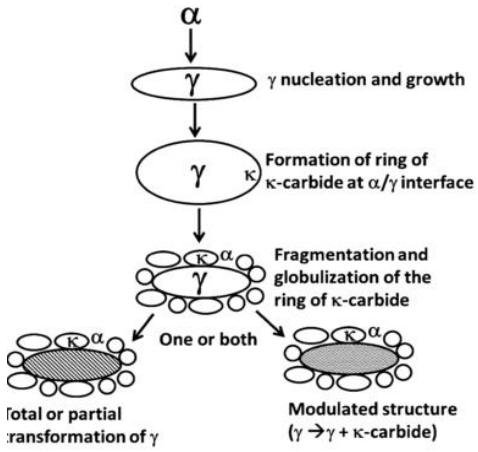

Fig. 1 The sequence of the phase transformation which is involved in formation of k-carbide [17].

1.1.6 Steels classification based on strength and ductility enhancing mechanisms

Precipitation hardening, solid solution strengthening, strain ageing, etc are some of the strengthening mechanisms. TWIP, TRIP, SIP are some of ductility enhancing mechanisms by which ductility increases because of plastic region instability delay. These mechanism enhances strength of steels by increasing work- hardening rate.

Precipitation-Hardenable Steels

k-carbides formation is main reason for precipitation hardening in LDS. In austenite and ferrite matrix, these k-carbides provides strength. Carbon in Fe-Al-Mn-C is alloying element to form k-carbides [3]. During ageing, k-carbides precipitates at around 500-750^{0}C.

TWIP Steels

The transformation of austenite to martensite occurs when strain is induced in any body and the stacking fault energy is less than about 20 mj/m^2. Austenite is deformed by twinning when amount of stacking fault energy is less than above amount. The extra elongation is due to delay in start of plastic instability during tensile deformation. TRIP effect was reported in low manganese containing duplex steels (e.g., Fe- 3.5Mn-5.8Al-0.35C by wt. %). It was found that TRIP effect was dependent was also found to be dependent on the annealing temperature in the inter-critical phase field because it controls the partitioning of elements in austenite and ferrite, and thereby the stability of austenite**.**

TRIP Steels

Manganese amount and inter-critical annealing are parameters which determines TWIP effect in low density steels [18]. The dislocations and stacking fault movement are restricted by coherent twin boundaries which acts as a restriction same as grain boundaries [19]. Austenite to hexagonal martensite transformation is suppressed by adding aluminium in Fe-Mn-Al-C alloys, so deformation occurs by twining mechanism. Addition of aluminium beyond a limit founds to reduce the twin density in Fe-30Mn-7Al-0.95C (wt. %) alloy because aluminum increases stacking fault energy [20]. Austenite deforms to martensite by planar glide when stacking fault energy of austenite is low and when it is high, the deformation mechanism is wavy glide rather than planar glide.

CHAPTER 2 LITERATURE REVIEW

The literature review part is divided mainly into two sections, early works and recent works. Early works is concerned about evolution of the system. This deals with the earliest research and how the researchers looked upon it. The recent works are more related to the research which was performed in within two decades.

2.1 Early works

The use of aluminium in steels is not a new concept. Aluminium was used in steels as deoxidizer before World war II [21]. In 1887, Robert A. Hadfield had patented a steel's group which contains aluminium from 0.1 to 20 wt. % Al [22]. He also done few experiments to study effect of aluminium addition in Iron-Carbon alloy with content up to 5.6 wt. % [23]. He had produced material with higher aluminium content (9.14 wt. %) but complete study was not done. At that time Fe-C phase diagram was yet not published and use of names like ferrite and pearlite were just started. Hadfield's conclusions were not on effect of aluminium addition on structure but on fluidity forging, fracture test, etc. Hadfield concluded that aluminium addition has not much effect on melting point.

When proper phase diagrams were established, then investigations on high aluminium added steels were started. Identification of microstructure components [24], determination of phase stability [25], and mechanical properties were studied. After 1980, replacement of Ni-Cr stainless steel with austenitic alloys of the Fe-Mn-Al-C system was forecasted. In the mean time period research on evolution of microstructure on rapidly solidification of alloys was conducted [26] and later on two phase austenitic-ferrite microstructure [27].

Table 1 Effect of different elements [29].

Element	Pros	Cons
Al	Forming Protective layer of Alumina	Forming FeAl and Fe_3Al which will lower the ductility
C	Stabilizes Austenite	Carbides may form at temperature higher than 500 °C
Mn	Stabilizes Austenite	The high Mn content will result in formation of β-Mn that lowers ductility
Si	Improves formation of Alumina layer	Hinders the continuity of the Alumina Layer
Ni	Stabilizes Austenite	Expensive, and lowers the uniformity of the protective layer.

Frommeyer et al. from Max-Planck-Institute fur Eisen forschung GmbH (MPIE) in late 1990 were first to discuss the reduction of density as function of aluminium content for binary Fe-Al alloys as shown in Fig.. This study since then had set important design parameters for the development of LDS for automotive applications in Europe because of strict regulations set by European Union concerning carbon dioxide emissions in coming years.

Sato et al. published their work in 1988 and discussed about age hardening behavior of Fe-Mn-Al-C alloy system. In their work they first solutionized the samples at 1273 K (1000 ℃) for one hour and then performed the ageing in a salt bath at 823 K (600 °C) [10]. After this they searched for the signs of the spinodal decomposition in the samples undergone ageing. The tests they used are composed of a hysteresis loop, bright field image of a 30 min aged sample along of its electron diffraction pattern; which the presence of satellites is a proof of the existence of fluctuations in composition which may be the results of the spinodal decomposition.

Ishida et al. [14] in 1990 had done important work by studying and exploring the phase diagram and equilibrium of phases in alloy system. The author studied the phase equilibrium of phases at different content of aluminium (0-10 wt.%) and manganese (0-30 wt.%) in the system. The Table 2 Effect of different elements [29].

main aim of the study was to clarify formation of k phase.

2.2 Recent work

The recent work is study of published work in last two decades. In the recent times with the advancement in sintering technique, the synthesizing process of low density steel has been shifted to powder metallurgy route. The published work reported superior mechanical properties.

Stefano Gialanella studied the effect of ball milling on Fe-40 at. % Al powder in 1985. He found that long range ordered phase disappeared. It shows the transformation from long range to short range phase. The lattice parameter increased by 0.8%. There is decrease in crystallite size and increase in lattice strain. Disordered intermetallic and their phase stability at high temperature is requirement in nuclear industry.

Yoritoshi Minamino et al investigated the microstructure and mechanical properties of bulk nanocrystalline made by mechanical alloying with subsequent spark plasma sintering in 2003. They produced three bulk nanocrystalline with varying carbon percent. They consolidated sample at 1073-1273K under 64MPa by SPS. The result were superior in terms of mechanical properties. The compacts with 1 and 2 at. %C of this work perform the superior mechanical properties (e.g. yield strength of 2150 MPa and rupture strain of 0.14 for compact with 2 at. %C at R.T.) when compared with the ordinary Fe_3Al casting (e.g. the yield strength of 380 MPa and rupture strain of 0.12). The compression test result is shown Fig.2.

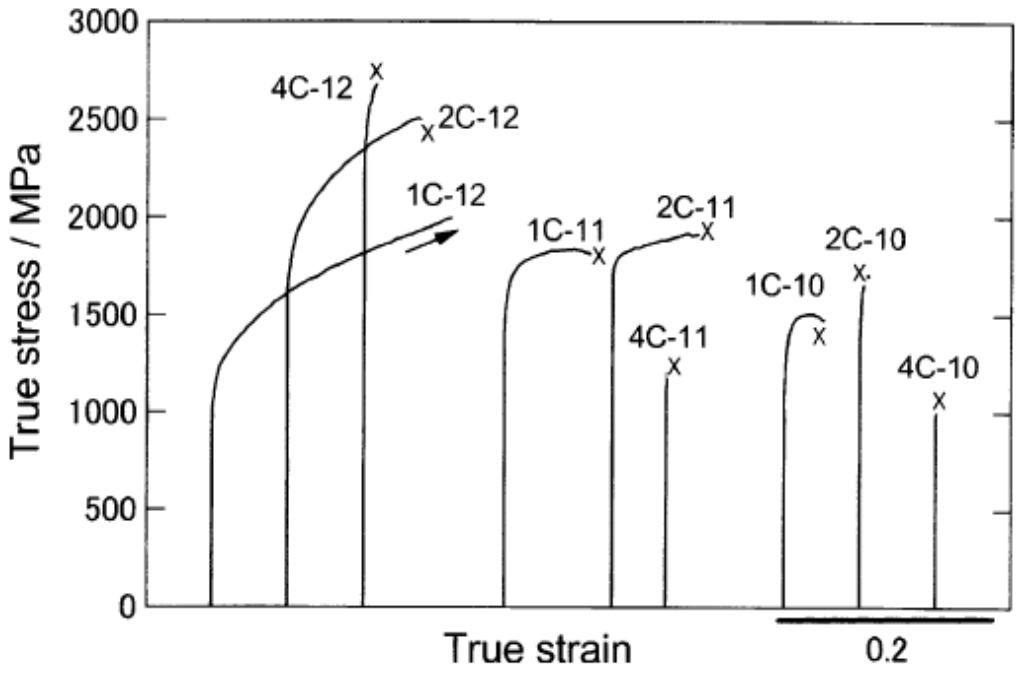

Fig. 2 True stress-strain curves of the Fe–Al–C compacts consolidated at 1073-1273K for 300s under 64MPa pressure. The compression was carried out at strain rate of $1.67 * 10^{-4}$ sec^{-1} [30].

Tomas Skiba, et al. applied the SPS to produce specimens from gas atomized Fe-43%Al powder in 2010. After optimizing sintering parameter, specimens were produced at that parameters. They found that sintering temperature below 950°C was not sufficient to provide complete densification of the material. When viewed from fracto graphic point of view, there is change in fracture phenomenon from interparticle decohesion to mixture of interparticle decohesion and transgranular decohesion with predominance of interparticle decohesion was observed with increasing sintering temperature from 950°C to 1000°C.

D. Raabe et al. investigated the influence of Al content and precipitation state on the mechanical behavior of austenitic high-Mn low density steel in 2012. They investigated strain hardening of two steels with aluminium content 2.1 wt. % and 8 wt. % respectively. They found that precipitation of intergranular M_3C type carbide strongly influence the fracture mode. They also found that strain hardening behavior of alloy with high aluminium content is associated with precipitation of shearable nano-sized k-carbides.

2.3 Literature gap

Aluminium is added to reduce density of steel but problem of loss of ductility occurs due to formation of intermetallic. Toughness also decreases significantly and formability of steel with high aluminium content restricts its application in automobile industry. The problem can be countered by addition of alloying elements like manganese which restricts formation of brittle intermetallic. Another problem in synthesizing low density steel by casting route is grain growth and formation of formation of precipitates at grain boundaries. This problem can be countered by sintering and forming bulk by using advanced sintering technique like spark plasma sintering in which due to rapid heating and cooling, the grain growth is restricted and advanced mechanical properties can be obtained.

CHAPTER 3 SYNTHESIZING PROCESS OF LDS

Low density steels can be synthesized either by melting process or sintering process. Both the process shows different mechanical properties and microstructure. The sintered bulk have advanced properties than casted bulk.

3.1 Synthesis of low density steel by melting process

The advancement of technology led to development of various advanced furnaces like vacuum induction melting, vacuum arc melting for formation of alloy materials with chemical and mechanical homogeneity for advanced applications.

3.1.1 Vacuum arc melting

Arc melting is applied to melt metals to form alloys with great homogeneity. The heating of material takes place through an electric arc which is struck between a tungsten electrode and metals placed in a depression (crucible) in the copper hearth. Melting is performed in argon atmosphere. Re-melting can be done to improve quality of alloy of bulk prepared by vacuum arc melting. Nickel, Titanium, steels are processed by this process. This technique has several advantage over traditional method:

- Solidification rate of material can be controlled more preciously than convectional technique.
- In open furnace, various gases like nitrogen, hydrogen, and oxygen are dissolved which has detrimental effect on alloys whereas in vacuum conditions, these gases escapes to vacuum chamber from liquid metal.
- Vacuum arc melting can be used to melt that material which are unable to be melted in open furnaces.

3.1.2 Basic principle of VAM

A standard Tungsten Inert Gas (TIG) welding unit is used as a power source. Heat generated by the electric arc struck between the electrode and the metals is utilized to melt the metals which are placed in the crucible to form an alloy. Repeated melting is performed to improve the homogeneity of the alloy. Evacuation of the chamber avoids oxidation of the melt (Ar being an inert gas does not react with molten metal).

3.1.3 Features of VAM

The metals can be heated to a temperature in excess of 2000ºC. A batch of five alloys can be made in a single evacuation, as there are five crucibles in the hearth (four small and one large). About 15g of metals can be melted in the small crucibles and about 80g in the larger crucible. There are three main parts to the system: power source (TIG– 600Amp), chiller and vacuum unit. The vacuum unit with rotary and diffusion pumps can attain a vacuum of 10□6 m bar. The cold circulation water from the chiller cools both the copper hearth and the electrodes. After elemental metals (or master alloy) are melted and solidified, it can be 'turned over' by a 'tweezer mechanism' without breaking the vacuum (and then re-melted). The melting → solidification → 'turn over' of sample → re-melting process is typically repeated three times to attain a better compositional homogeneity. Apart from the abovementioned hearth with five crucibles, an additional hearth has been provided with one crucible, which can suction cast the molten alloy, in the form of thin cylinders (typically 3mm diameter).

Fig. 3 Arc Melting Unit [4].

3.2 Synthesis of LDS by Sintering process

This process belongs to powder metallurgy in which powder is sintered to form bulk. The whole process is divided mainly into two parts namely alloy formation by mechanical alloying and then consolidation of alloy powder.

3.2.1 Mechanical alloying

Mechanical alloying is technique of formation of alloy phases by using mechanical energy from high energy milling in which repeated cold welding, fracturing and rewelding of powder particles takes place. Equilibrium and non-equilibrium alloy phases can be synthesized from pre-alloyed powders using this technique. In recent times, it is one of the most popular non-equilibrium processing technique used in production of advanced materials. This technique can be used to form super saturated solid solutions, crystalline and quasi crystalline intermediate phases, and amorphous alloys [21].This technique can be applied to metals, ceramics, polymers, and composite materials.

3.2.2 Historical background of mechanical alloying

It might be stated that this process was developed by Benjamin and co-workers and was referred as milling and mixing but the term mechanical alloying was coined by Ewan C. Mac-Queen, a patent attorney for INCO after that term was maintained in literature. The production of ODS GV-hardened super alloys requires dispersion of fine oxides can be achieved by milling of powder. The commercial application of any alloy requires certain characteristics such as full

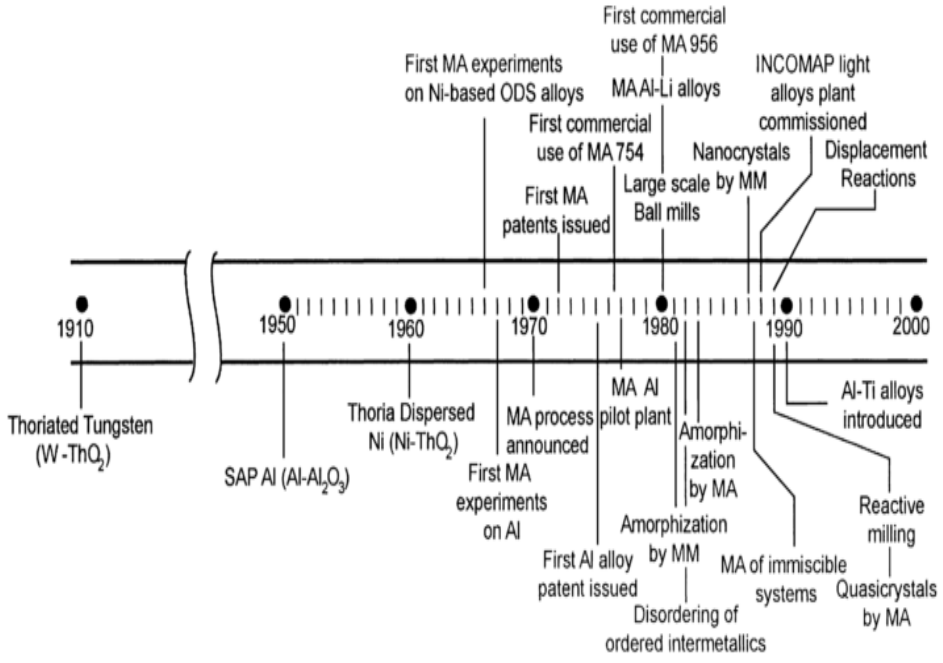

Fig. 4 Chronology of development of MA

densification, desired microstructure, desired properties. The desire of these characteristics had led to development of mechanical alloying. Excellent materials with advanced properties are synthesized using mechanical alloying as first step.

3.2.3 Equipment used for mechanical alloying

Raw material: The raw materials which are used in mechanical alloying are commercially available powders having size in range of 1-200 micrometre. The size of powder to be milled is not critical but it should be less than ball size which are to be used for grinding. The reduction of power size in milling follows exponential path. Few micrometre size of powder can be achieved within short interval of time. The raw powder which is divided into pure metal, master alloys, prealloyed powders, are milled for getting desired properties to be obtained.

Planetary ball mills: The use of planetary ball mills is done where fine powder upto nano scale is required. Besides size reduction, these mills have been found suitable for colloidal grinding and also provide energy input for mechanical alloying.

Fig. 5 Retch planetary ball miller [7].

Grinding medium: The selection of grinding medium on basis of its size, nature, and size distribution is a significant step in order to achieve effective milling of powders. The selection depends on analyzing interrelated

Specific Gravity: Generally, better results are obtained using high density media. High density mills have higher kinetic energy and thus higher energy will be transferred to the milled powder. The density of medium should be higher than the powder to be milled.

Initial Feed Size: The size of grinding medium should be larger than the initial feed size because smaller particles should not be able to break up large particles.

Final Particle Size: When fine particle size is desired then grinding medium should be smaller in size. The grinding medium should be smaller when very fine particles are desired; the smaller the grinding medium, the smaller is the final particle size.

3.2.4 Process Variables in Mechanical Alloying

There are various variables on which mechanical alloying depends and these variables have important influence in order to achieve desired product phase, microstructure, and properties. The nature of phase (solid solution, intermetallic, or amorphous phase, etc) formed will depend on process variables. For a given composition of the powder, some of the important variables that have an important effect on the final properties of the milled powder are as follows:

Type of mill: Various types of mills are employed for mechanical alloying. These mills differ in some important parameters like capacity, maximum speed of operation, temperature variation capability and the extent to which contamination is minimized

Milling speed: Faster rotation of mill imparts higher energy input into the powder. The reason behind this is the direct relation between speed and kinetic energy. Higher speed supplies greater kinetic energy to powder. There is certain limitation like design of grinding medium in setting maximum speed. Various disadvantages are associated with milling at high speed. The temperature rise during milling is higher during milling at high speed which results in decomposition of intermetallics and grain growth of powder particles. Excessive wear of tools also occurs due to high speed milling.

Milling time: This is important parameter in milling the powder. The time is set to such a value at which a steady state is achieved between fracturing of powder and cold welding of powder. This facilitates the mechanical alloying. The times required is related to other parameters like BPR, temperature of milling. The value should be chosen taking the consideration of other parameters also.

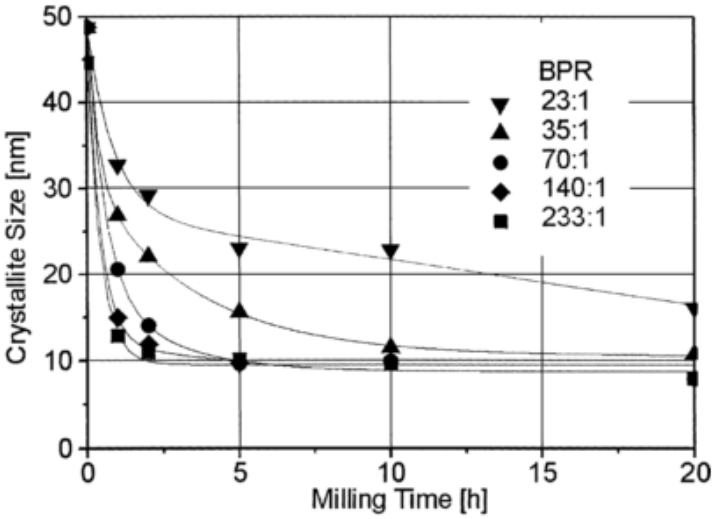

Fig. 6 Variation of .crystallite .size with .milling time and ball-to-powder wt. ratio (BPR) [20].

Ball-to-powder weight ratio: Ball to powder ratio is the ratio of total weight of balls to that of weight of powder. Many researchers had studied the impact of BPR on properties of milled powder and concluded that ratio should not be higher than 1000:1 and shouldn't be too low. Very high values are irrelevant. The ratio of 10:1 is mostly used during milling of powder in small capacity. Higher energy ball mills requires low BPR and vice versa with low energy mills like an attritor, in which BPR of as high as 100:1 occasionally used in order to achieve desired result.

Milling atmosphere: The atmosphere of milling is very vital during mechanical alloying. MA is normally conducted under vacuum or in inert gas atmosphere in order to prevent contamination and oxidation of powder. Contamination and oxidation degrades properties of powder and create hindrance during further processing of powder. Inert gases like argon is used. Nitrogen is not widely used because it has tendency to form nitrate phases which contaminates powder.

Process Control Agents: Process control agent plays significant role during milling of ductile powder as they are prone to large plastic. The plastic deformation causes welding of powder with grinding medium. PCA prevents welding of too much powder with grinding medium so that homogenization will takes place throughout the powder. PCA maintains balance between fracturing and welding. PCAs can be solid, liquid, or gaseous. They are mostly, but not necessarily, organic compounds, which act as surface-active agents. They get adsorbed on the

particles' surface and in this way minimize cold welding among particles of powder, thus reduces probability of forming agglomeration.

3.2.5 Mechanism of Mechanical Alloying

The mechanism of MA is different for milling of ductile powder and brittle powder. Plastic deformation is large in ductile powder so welding is more in that powder. The repeat ion of fracturing and welding causes the mechanical alloying. In ductile-brittle combination the ductile powder is flattened and brittle powder is fragmented and get trapped into ductile powder

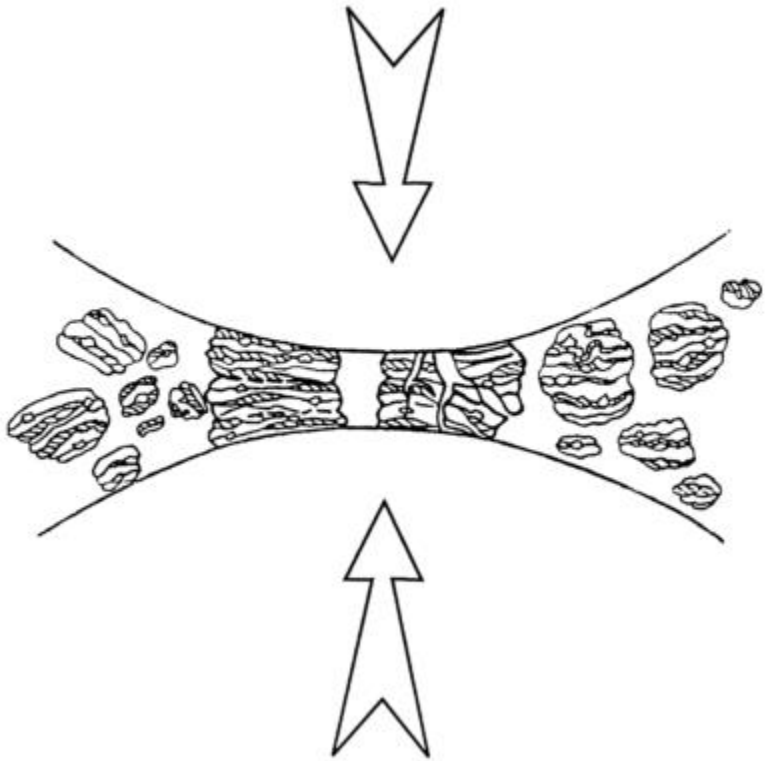

Fig. 7 Mechanism of fracturing and rewelding [21].

3.3 Consolidation of powder

The consolidation of powder to form bulk is termed as sintering. Sintering process involves making of object from its powder. Powder is heated in furnace below its melting in order to facilitate diffusion of atoms so that bonding can takes place. Individual particles adheres with surrounding particles to form dense compact. Convectional sintering, spark plasma sintering, Microwave sintering are some of methods involves in sintering of material.

3.3.1 Spark plasma sintering

Spark plasma sintering is technique of consolidation of powders in which pulse electric current is utilised to sintering or joining the individual particles in powder. SPS is a rapid sintering technique in which the heating of powder takes place entirely over volume of powder homogenously at macroscopic level. The heat which is generated by joule is dissipated at individual powder locations at microscopic levels, where energy is required for sintering, i.e. at contact points. This gives advantage of low grain growth and suppressed powder decomposition. The direct way of powder heating allows high heating rates and high cooling

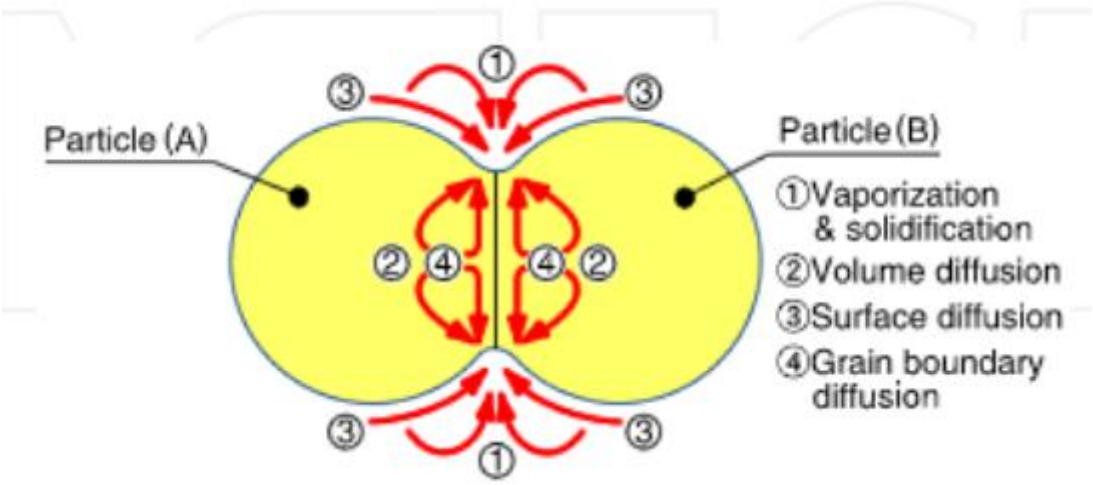

Fig. 8 Material transfer path during sintering [15].

rates which ultimately suppress grain growth and enhance densification by promoting diffusional mechanisms as shown in Fig 8.

3.3.2 The basic SPS configuration

The basic configuration of typical SPS is shown in Fig.9. The SPS system contains a SPS sintering machine which has feature to apply pressure from singe vertical axis. It has in- built water-cooled special energizing mechanism, a water-cooled vacuum chamber, atmosphere controls, vacuum exhaust unit, special sintering DC pulse generator and a SPS controller. The powder of the material which is to be sintered is kept in between die and punch in the chamber and is held between the electrodes. The temperature quickly rises to 1000-2500^{0}C under applied pressure. This results in high quality product in short span of time.

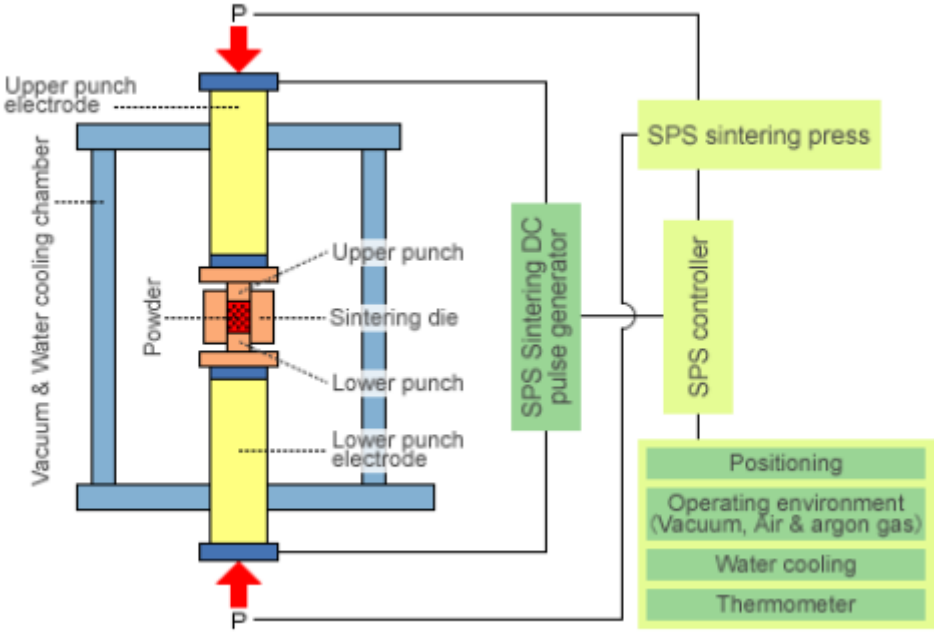

Fig. 9 SPS system configuration [14].

3.3.3 Principle of SPS process

The main principle behind SPS process is electrical spark discharge phenomenon in which a high energy low voltage pulse current generates plasma at high localized temperature ranges from seven to ten thousand degree Celsius at contact points of particles which gives driving force for thermal and electrolytic diffusions. The time required for vaporization, melting and sintering is small, in range of 5 to 20 minutes, including temperature rising and holding time. Various theories for effect of SPS have been proposed:

Plasma generation

Inoue and inventors of SPS process claimed that pulse current generates sparks and even plasma discharges between particle's contact points, which was main reason for naming this process as spark plasma sintering and plasma activated sintering [25]. They claimed that "Impulsive pressure" was developed due to ionization at contact points of powder which facilitates diffusion of atoms at contacts. Groza et al, studied grain boundary region of bulk formed by SPS and found that grain boundary region is oxidation free which implies that pulse current has cleaning effect on particles surface.

Joule heating

Current which flows through the powder generates heat which is utilized in welding of particles in presence of mechanical pressure. Due to intense joule heating, the conducting surface of particles often reaches to its boiling point and thus localized vaporization or cleaning of powder surface takes place.

Mechanical pressure

Application of mechanical pressure increases the contact of particles and in this way diffusional distance of atoms get reduced and enhance the bonding.

3.3.4 Mechanism of SPS

The mechanism of neck formation in spark plasma sintering is divided into five main stages.

Initial stage

In this stage, spark discharging takes place by ON-OFF pulse energization.

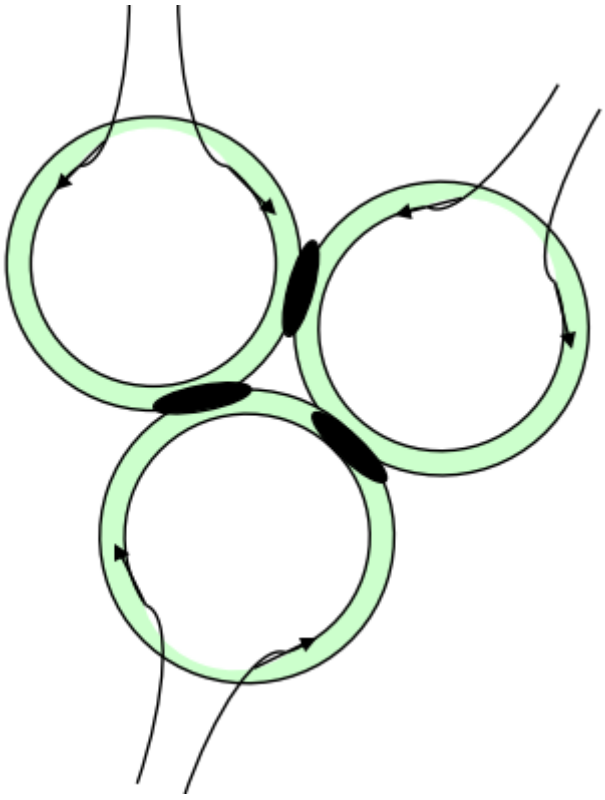

Fig. 10 Mechanism of neck formation in SPS [19].

3.3.6 Process variables of SPS

There are various process variables on which desired properties of the product depends. These variables need to be optimized to get good densification, microstructure and other mechanical properties. Some of important process variables which have significant influence on product are explained below:

Effect of heating rate:

Heating rate effect has been investigated thoroughly in many research works both in pressure and pressureless sintering. Enhanced densification is observed in pressureless sintering because mechanism which are not involved in densification are by-passed and also due to creation of large thermal gradient [20]. In many recent publications on **s**tudy of heating rate effect, the result is that heating rate (between 50^{o}C to 700^{o}C) have no effect on final density of sintered sample at same temperature and at same length of time. In publications related to work on microscopic and Nano metric size powder, it was found that an increase in heating rate has no effect on final density in microscopic size powder but in nano size powder, an increase in heating rate decreases the final density. The explanation given by author is that there is existence of large thermal gradient with high heating rate.

Effect of pressure:

Pressure is applied to achieve higher densification at same temperature. Pressure plays mechanical as well intrinsic role. The mechanical role of pressure is on particle rearrangement during sintering and breaking of agglomerates in case of nano scale powders. The significance of pressure depends on particle size of powder. When powder size is small pressure has little influence but when particle size is large pressure has significant influence. The effect of pressure in achieving 95% density is shown in Fig.11. When applied mechanical pressure increases, the temperature required to achieve desired density is lesser. As a result, the grain size in sintered product is small which is extra advantageous for good mechanical properties. At lower pressure, high temperature is required to achieve desired densification. The high temperature produces deteriorating effect such as grain growth, chances of melting of powder, etc. Desired densification at lower temperature is always desirable in sintering.

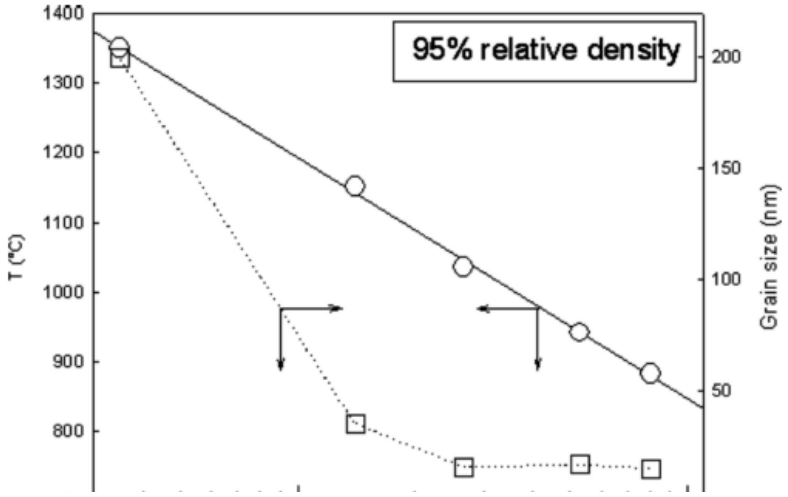

Fig. 11 Effect of .pressure on the .temperature needed to .get 95% relative density for .cubic ZrO2. The .corresponding decrease in grain size .is also shown [22].

Role of current

The role of current in SPS is like function of brain in human body. Current cause joule heating which cause diffusion of atoms and hence densification is achieved. Current also has role of creating plasma. Plasma causes cleaning effect on surface of particles and this enhanced sintering. Current also have effect on mass transport. The influence can be manifested through the electron wind effect (electro migration) [46], or by an increase in point defect [48], or by a decrease in the activation of migration of the defects [49]. This effect must be isolated from joule effect.

3.3.7 Advantage of SPS over Convectional sintering

- Heating and cooling rate are faster in SPS than in convectional sintering. In SPS heating takes place directly at powder but in convectional sintering, heat is transferred by radiation from furnace wall to the powder.
- Current gives cleaning effect on surface of particles which enhances densification.
- Due to fast process, grain growth can be suppressed which give advanced properties than convectional sintering.
- In SPS, the sputtering pressure generated by spark plasma removes adsorptive gases and impurities which is an advantage over convectional sintering.

CHAPTER 4 EXPERIMENTAL PROCEDURE

4.1 Material used

Iron, aluminium, carbon and manganese powders with 99.9% wt. % purity are mixed in respective composition shown in Table 2.

Table 2 Sample compositions and their respective names, all the values are in wt. %.

Sample name	Fe	Al	Mn	C	Theoretical density (g/cm^3)
1	Balanced	23	0	0.4	5.43417
2	Balanced	10	20	0.4	6.8347
3	Balanced	13	0	0.6	6.2426
4	Balanced	9	4	0.2	6.6714
5	Balanced	9	4	0.2	6.6714
6	Balanced	9	4	0.2	6.6714
7	Balanced	9	4	0.2	6.6717

4.2 Optimization of process parameters in SPS

For optimizing process parameters, trial and error analysis was done. The sample was prepared and then extent of consolidation was measured. If desired consolidation was not achieved then consolidation using SPS was repeated with varying parameters. The experiment was repeated until desired parameters were obtained.

4.2.1 Trial and error analysis

Sample 1

Mechanical alloying

Mechanical alloying was carried out using high speed retsch planetary ball mill. The grinding medium is of stainless steel. The composition of each sample is taken as indicated in Table 1.Sample 1 is mechanically alloyed for 12 hrs. The ball-to-powder ration kept was 5:1. The milling speed was 300 rpm. Toluene was used as process control agent. The milling was wet

and done in normal atmosphere. For sample 3, 4, 5, 6 there was slight change in process parameters as only milling time was increased to 50 hrs and rest parameters were kept constant.

X-Ray diffraction Characterization

The milled powder was characterized by analyzing the X-ray diffraction profile using Xpert software.

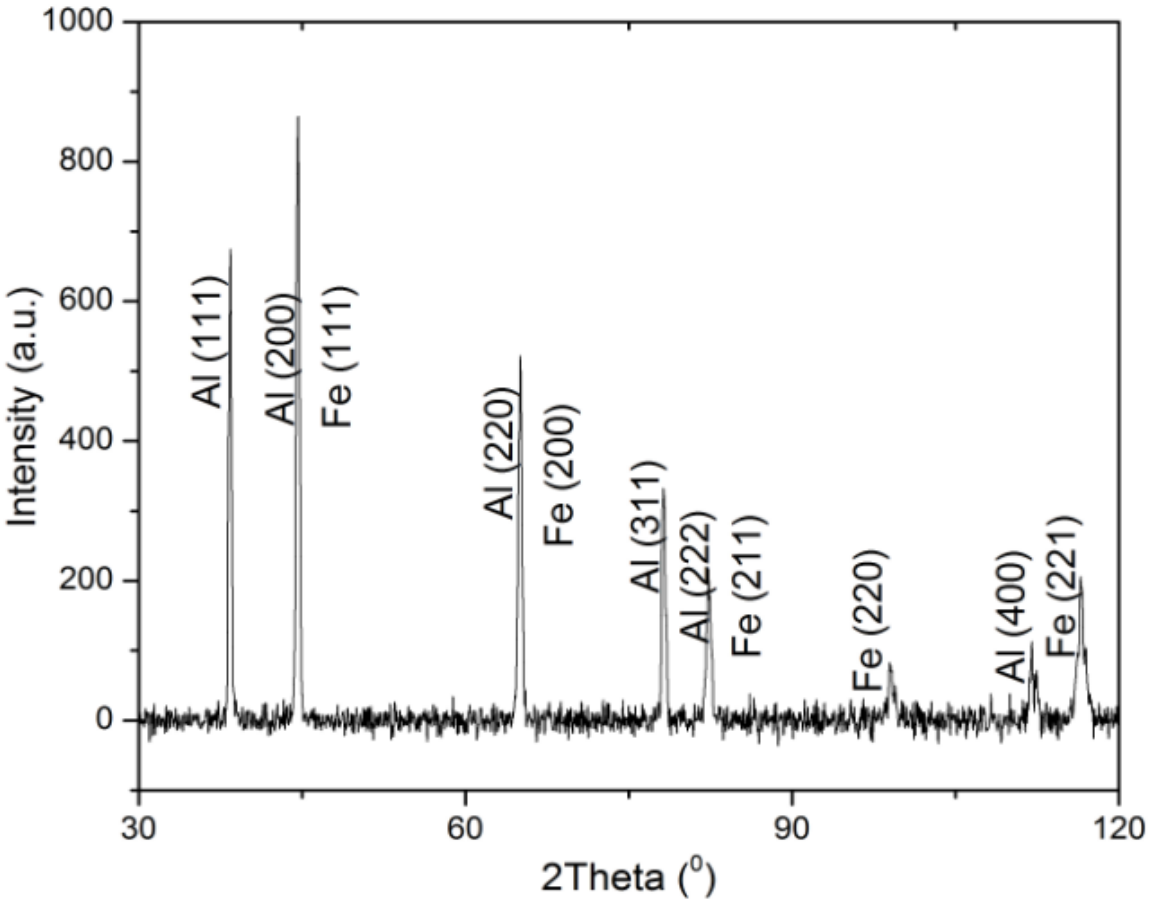

Fig. 12 X-ray diffraction profile of Fe–Al–C alloy powder.

The powder obtained after ball milling was consolidated into disc (20mm diameter, 5mm height) using cylindrical graphite die and punch by using Dr. Sinter SPS machine. Single stage sintering was done for sample 1. The process parameters of sample 1 are shown in Fig. 13. Sample 1 was sintered at 1050^0C. The pressure applied was 60 MPa. The holding time at sintering temperature was kept at 5 minutes.

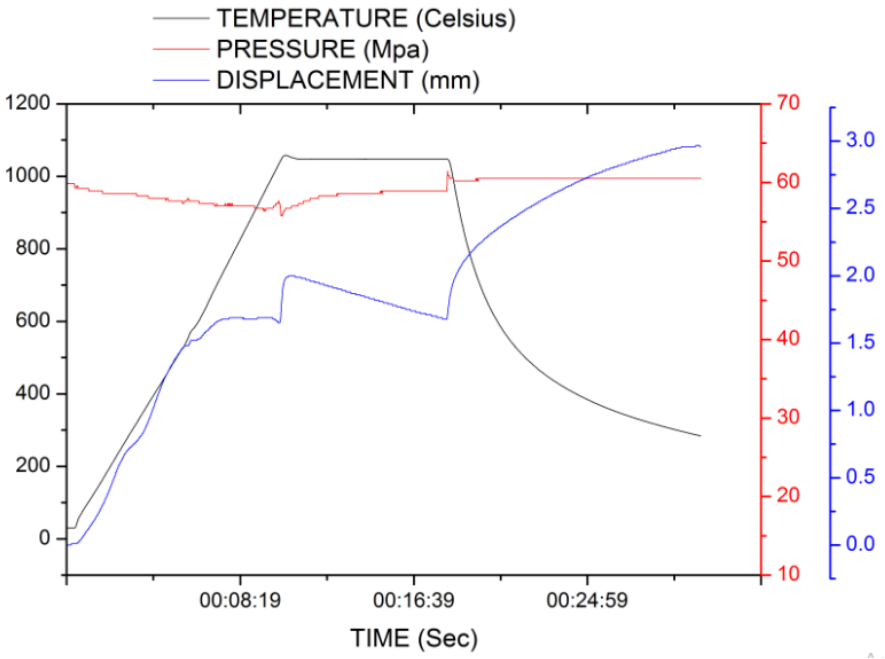

Fig. 13 Typical SPS cycle of sample 1 obtained from control panel of SPS showing different stages of sintering.

Microstructural characterization of sample 1

Microstructural images of sample 1 are taken using scanning electron microscope and are shown in given below.

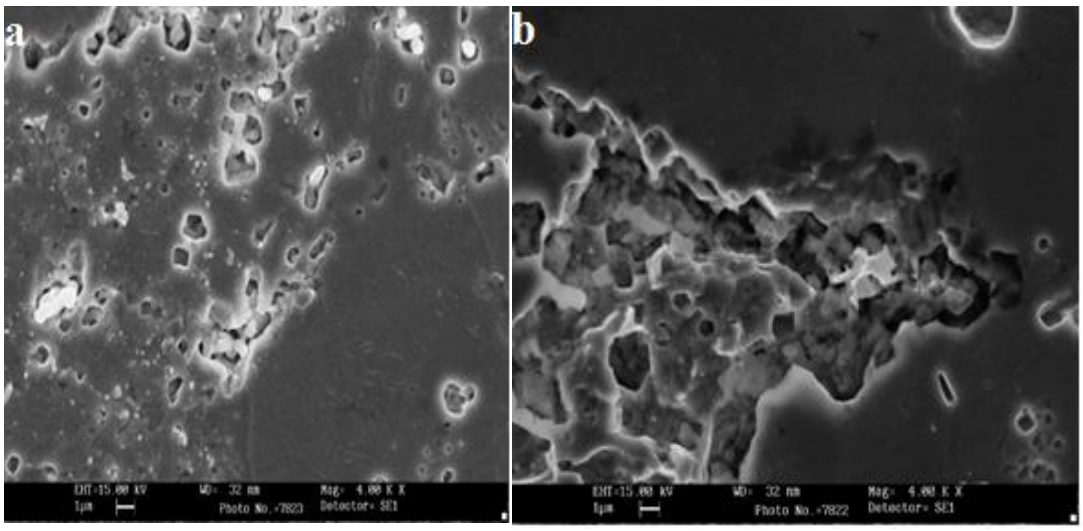

Fig. 14 SEM images of sample 1 at (a) Central position (b) Corner position.

Sample 2

Mechanical alloying

Milling time for sample 2 was increased to 40hrs. The BPR was increased to 10:1. The milling speed was kept at 300rpm. Toluene was used as PCA and wet milling was done. The X-ray diffraction profile was obtained for both as mixed and 40hrs milled powder and a comparison was made by plotting the two profile on common axis as shown in fig 15.

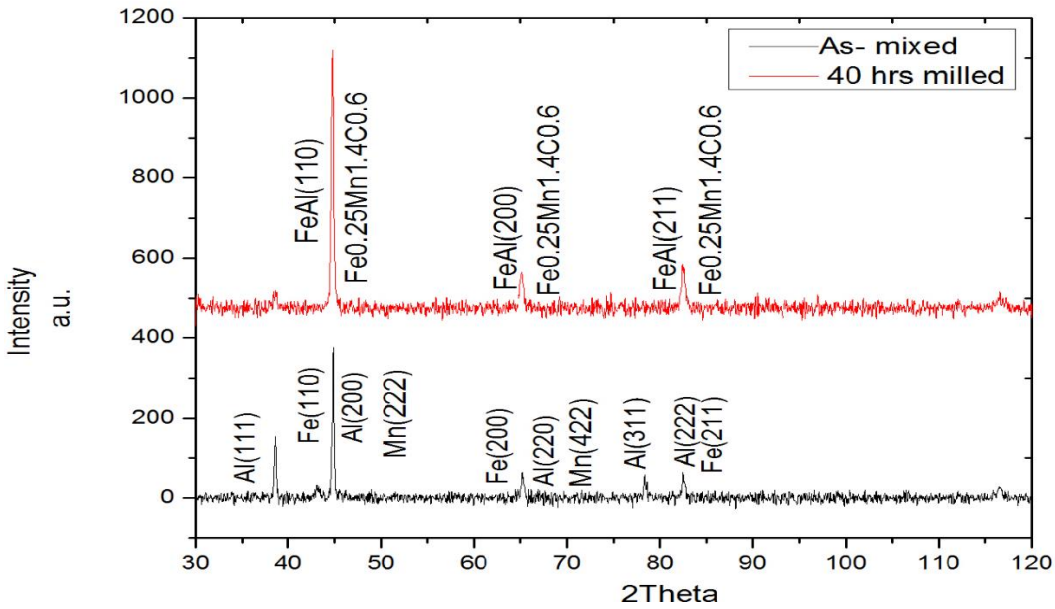

Fig. 15 Comparison of X-ray profile of powder of sample 2.

The process variables for sample 2 are shown in Fig. 16 . Pressure applied was taken as 60MPa. The sintering temperature and holding time were taken as 1050^0Cand 8 minutes.

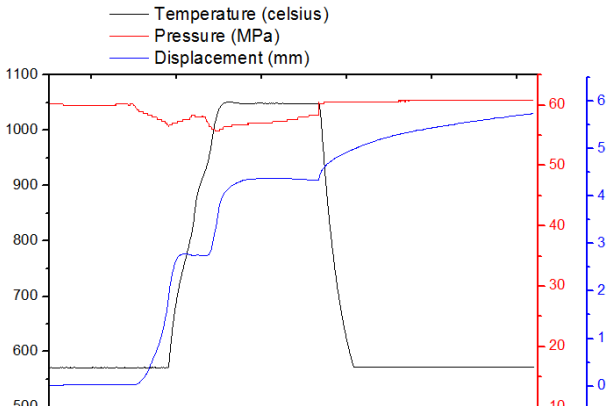

Fig. 16 Typical SPS cycle of sample 2 obtained from control panel of SPS showing different stages of sintering.

Microstructural Characterization of sample 2

The microstructure images taken using scanning electron microscopy are shown in fig

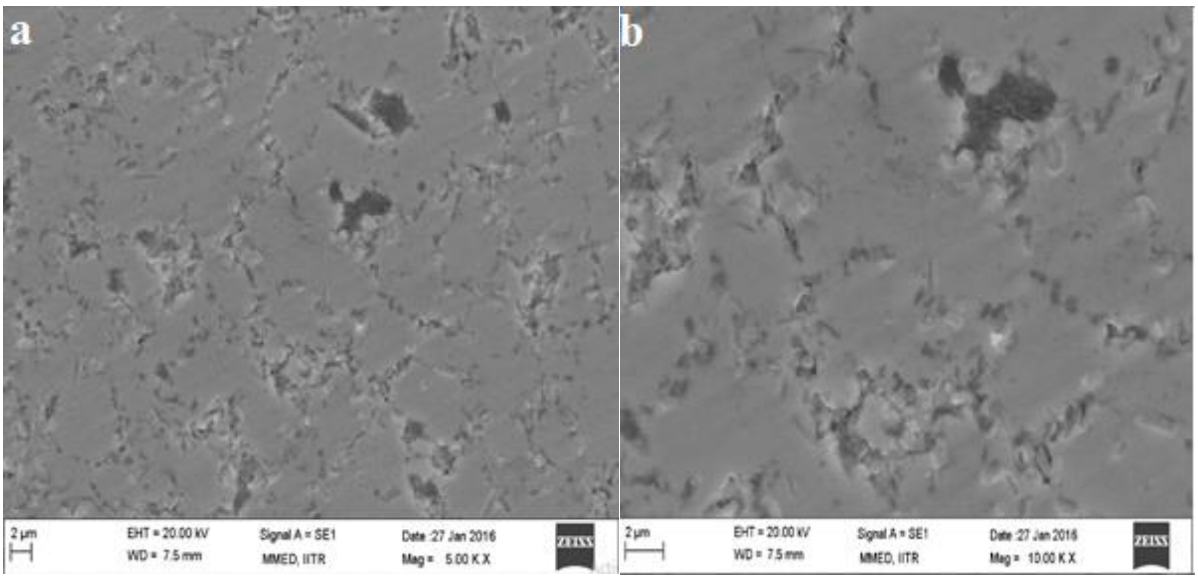

Fig. 17 SEM images of sample 1 taken at (a) 5KX (b) 10KX

Sample 3

Manganese was not mixed in sample 3. The process parameters except time which was increased for 10hrs for ball milling were fixed same as were in sample 2. Multi stage sintering was opted instead of single stage sintering with initial holding of 3 minutes at 550^0C. The sintering temperature was reduced to 800^0C with 5 minutes holding at that temperature. Pressure was taken as 60MPa.

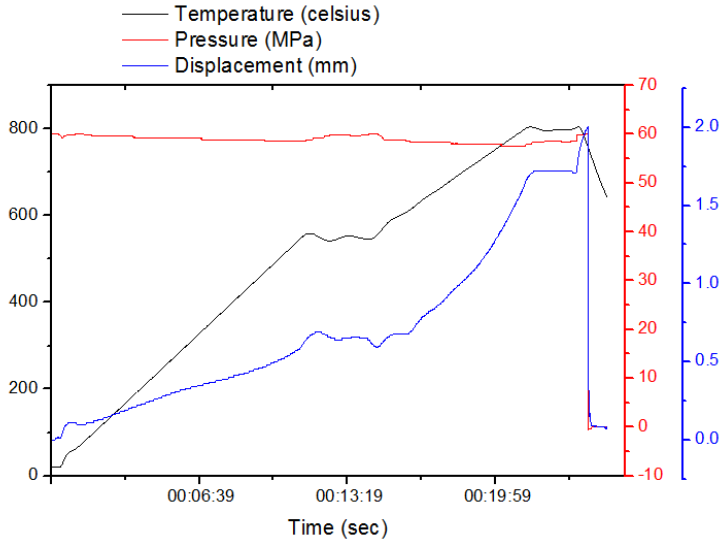

Fig. 18 Typical SPS cycle of sample 3 obtained from control panel of SPS showing different stages of sintering.

Microstructural Characterization of Sample 3

The microstructure of sample 3 was taken using scanning electron microscopy. The microstructure are shown in Fig.19

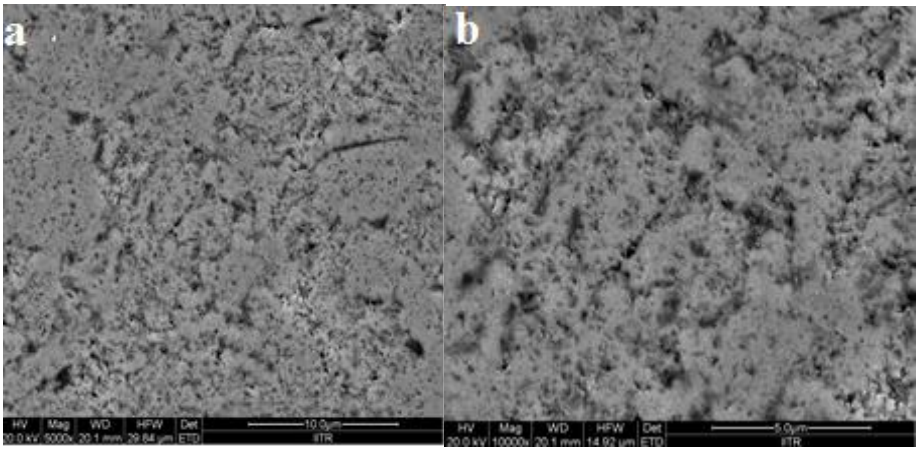

Fig. 19 SEM images of sample 3 taken at (a) 5KX (b) 10KX

.**Sample 4**

The process variables of sample 4 are shown in fig 20. Multi stage sintering with initial holding of 5 minutes and 3 minutes at 550^0C and 800^0C respectively. The sintering temperature was 900^0C with holding of 5 minutes. Pressure applied was 60 MPa.

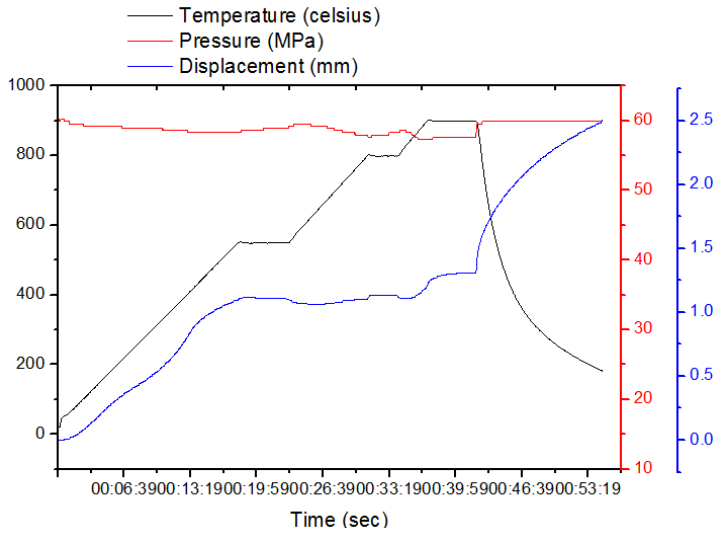

Fig. 20 Typical SPS cycle of sample 4 obtained from control panel of SPS showing different stages of sintering.

Microstructural Characterization of sample 4

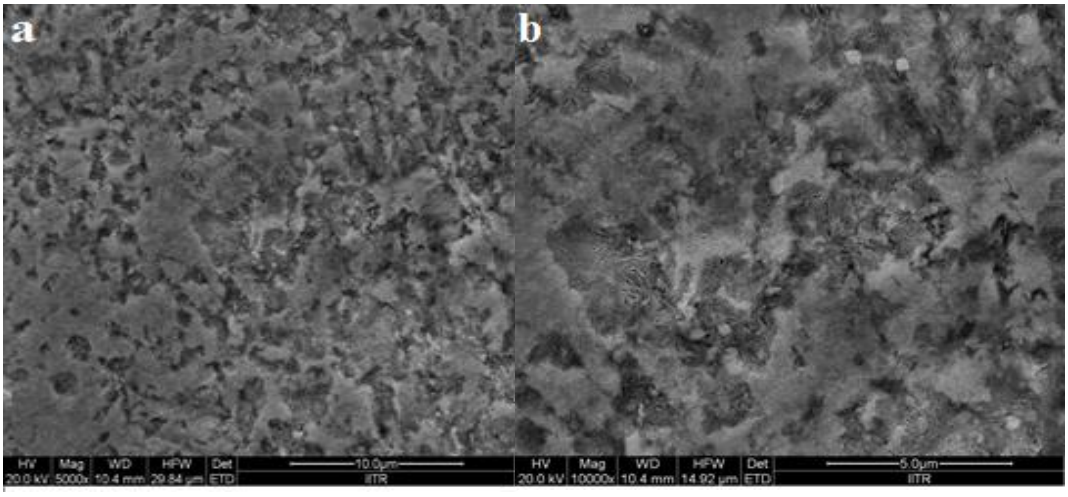

Fig. 21 SEM images of sample 4 taken at (a) 5 kX (b) 10 kX

Sample 5

The process variables of sample 5 are shown in fig 22. Multi stage sintering was done with initial holding for 5 minutes and 2 minutes at 550^0C and 800^0C respectively. Sintering temperature was increased to 1000^0C with holding for 3 minutes. Pressure applied was 60 MPa

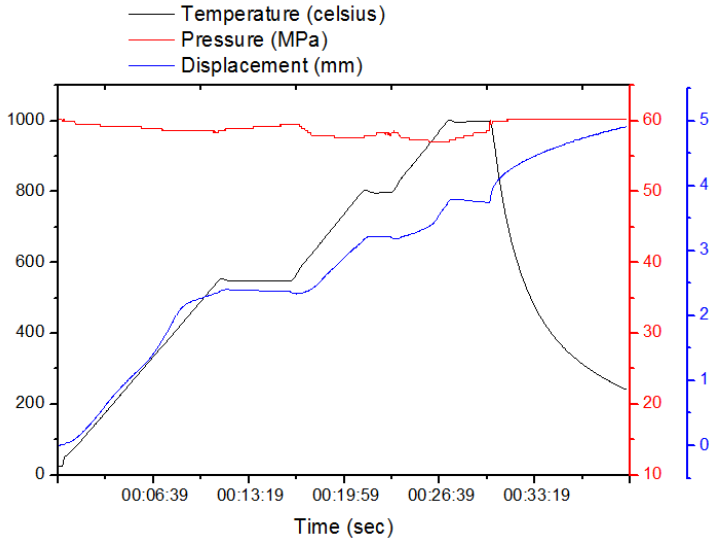

Fig. 22 Typical SPS cycle of sample 5 obtained from control panel of SPS showing different stages of sintering.

Microstructure characterization of sample 5

The microstructure of sample 5 was taken using optical as well as scanning electron microscope.

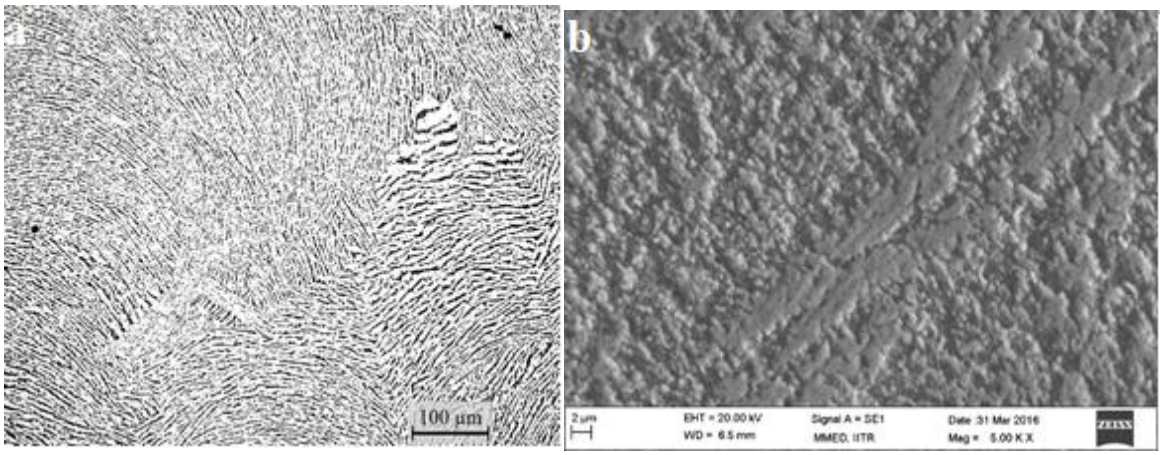

Fig. 23 (a) Optical microstructure of sample 5. (b) SEM microstructure of sample 5.

Sample 6

The process variables of sample 6 are same as that of sample 5 except an increase of 50^0C in sintering temperature. Multistage sintering was opted for consolidation of sample. The holding time is same as that of previous sample.

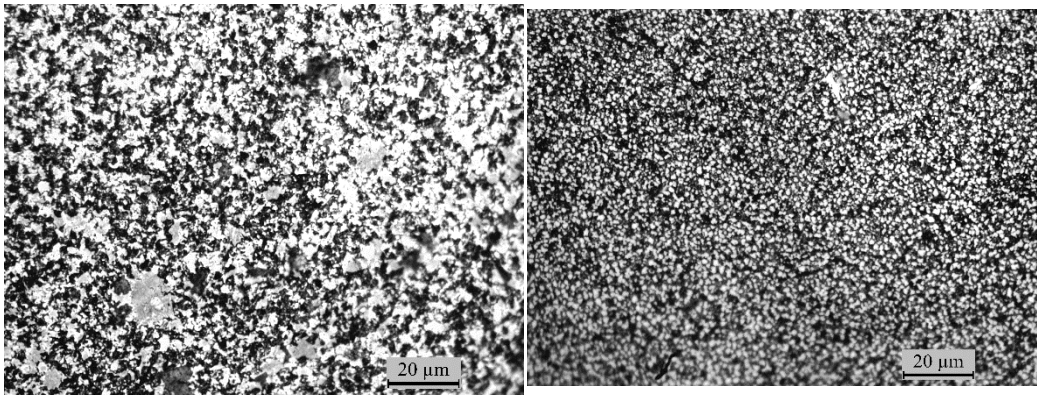

Fig. 24 Optical images of sample 6 sintered at 10500C.

Sample 7

Sample 7 was prepared via melting route. Green pellet was formed using hydraulic pressing with load of 15 ton. The pellet was then melted in vacuum arc melting furnace to form bulk.

Microstructure characterization of sample 7

The microstructure of sample 7 was taken using optical microscope. The optical images are shown in Fig.25 given below.

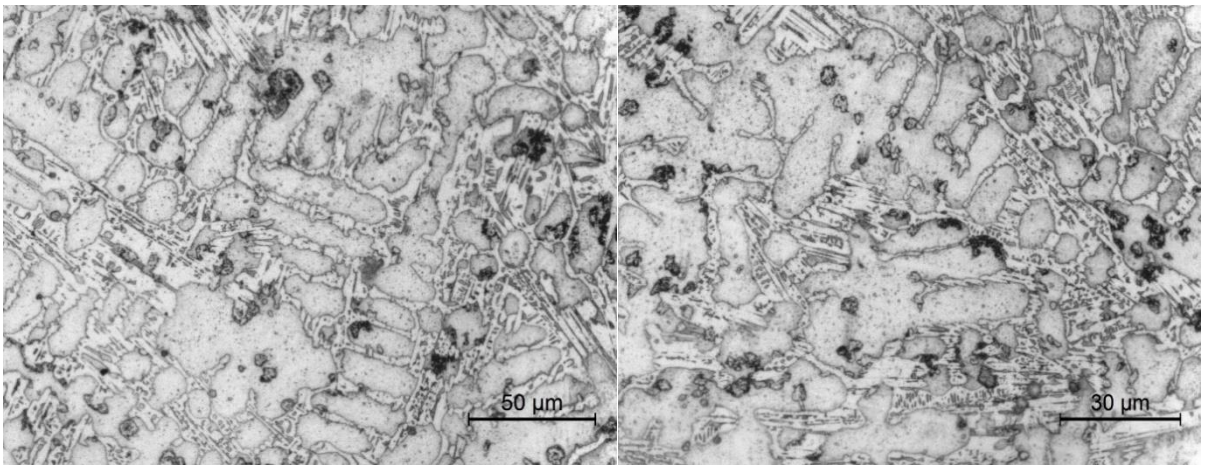

Fig. 25 Optical images of sample 7 synthesized by melting route.

4.3 Mechanical characterization of samples

4.3.1 Hardness

The hardness of sample all samples is taken using vicker hardness testing machine with 10kgf load and dwell time of 15 sec.

4.3.2 Compression test

The compression test was carried using Instron universal testing machine. Cylindrical sample was made from pellet obtained from SPS using EDM wire cutting. The dimension of sample were 9mm height and 6mm diameter. The speed of compression was .08013 mm/sec^{-1}.

CHAPTER 5 RESULTS AND DISCUSSION

5.1 X-ray diffraction analysis of milled powder

The x-ray diffraction of powder shown in Fig.13 after ball milling shows free peak of aluminium. This states that homogenous solid solution has not formed and free aluminium is still there. There is need to increase BPR and milling time for getting homogenous solid solution. So, milling time and BPR both were increased to 40hrs and 10:1 respectively. Comparison was made between milled powder and as mixed powder's X-ray diffraction profile as shown in Fig.16.

The formation of homogenous solid solution is clearly stated because free aluminium peaks get disappeared and intensity as well as broadening of peak increases which are the evidence of formation of solid solution.

5.2 Microstructural analysis of bulk samples

The microstructure of sample 1 shown in Fig.15 shows clear evidence of porosity. Different regions have different diffusion rates due to inhomogeneous distribution of elements. The microstructure of sample 2 shows porosity because of high manganese content and melting of material. Microstructure of sample 3 and 4 shown in Fig.19 and Fig.21 shows porosity which is almost uniformly distributed. This means temperature was not sufficient for diffusion and slightly high temperature is required for maximum consolidation. Porosity get minimized in microstructure of sample 5 as shown in Fig.23 because of increase of 100^0C in sintering temperature. The microstructure of sample 6 which was sintered at 1050^0C shows evidence of grain growth and increase in porosity due to high temperature. The microstructure of sample 7 which is the melted sample shown in fig 28, shows sign of dendritic growth. The grains are large as compared to sintered sample.

5.3 Phase Evaluation: Sintered vs Arc melted sample

Phase diagram was drawn using thermo-calc software for getting details of expected phases which will come when bulk will be made. The phase diagram is shown in Fig. 26. BCC_A2 and carbides precipitates are main phases expected in bulk.

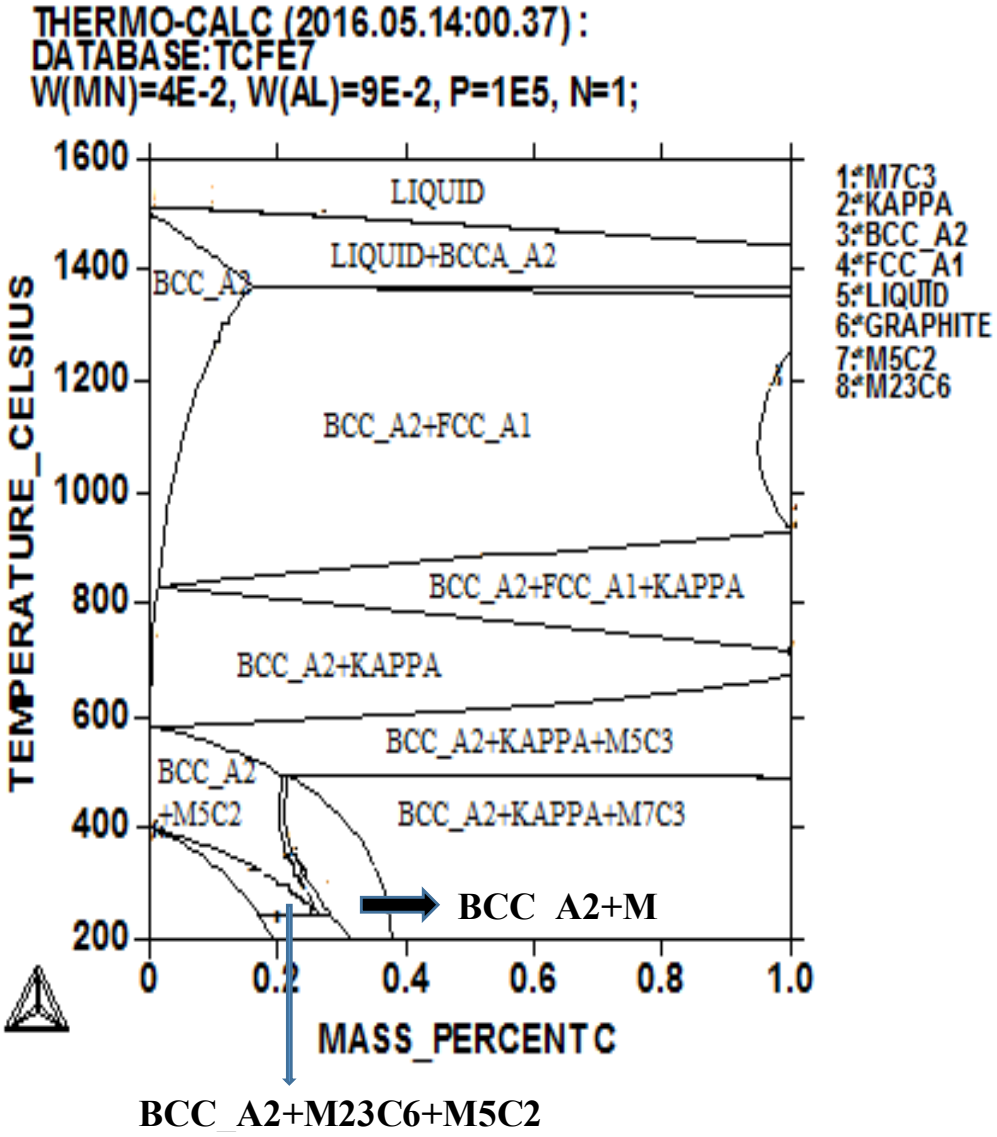

Fig. 26 Isopleth phase diagram drawn using thermo calc.

Actual phases present are evaluated by analysing x-ray diffraction profile as shown in fig below using X-pert high score plus software. When comparison between melted and sintered sample was made it was found that sintered sample's profile showing more peaks of precipitate which are responsible for its enhanced mechanical properties. K-carbide is main precipitate in sintered sample while manganese carbide is precipitate in melted sample. Melted sample's phases are more close as expected by the phase diagram drawn using thermo calc software.

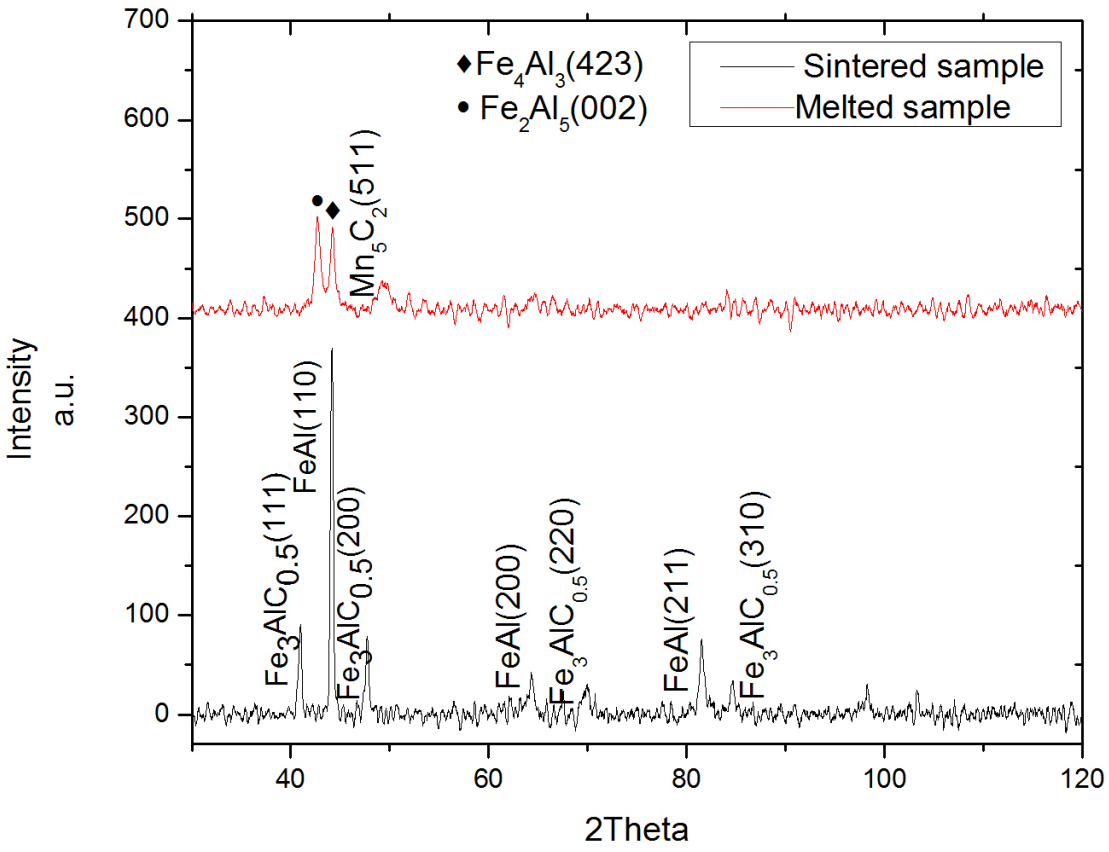

Fig. 27 Comparison of X-ray diffraction profile between melted and sintered sample.

5.4 Mechanical characterization

5.4.1 Hardness

The hardness of various samples obtained is shown in table 4 . It was found that sample 5 sintered at 1000^0C has maximum hardness value of 920VHN. Sample 7 which is synthesized by melting route has hardness value of 560VHN which is quite inferior when compared with sintered sample. Small grain size and large amount of precipitates due to rapid cooling in SPS is main reason behind the enhanced hardness. Melted sample has large grain due to grain growth which is main reason for low value of hardness.

Table 3 Hardness value of bulk sample prepared at various sintering temperature.

SAMPLE NAME	SINTERING CONDITION	HARDNESS VALUE
3	Temp-800^{0}C,pressure-60MPa	800VHN
4	Temp-900^{0}C,Pressure-60MPa	620VHN
5	Temp-1000^{0}C,Pressure-60MPa	920VHN
6	Temp-1050^{0}C,Pressure-60MPa	600VHN
7	Melted	560VHN

5.4.2 Compression Test

The true stress strain curve was obtained and shown in Fig. 28. The curve shows Ultimate tensile value of 2GPa with compressive strain of 22% at UTS. The 0.2% proof stress value is 1500MPa which is quite high when compared with literature. The large fraction of precipitate and small grain size in sintered sample is responsible for such a high compressive strength.

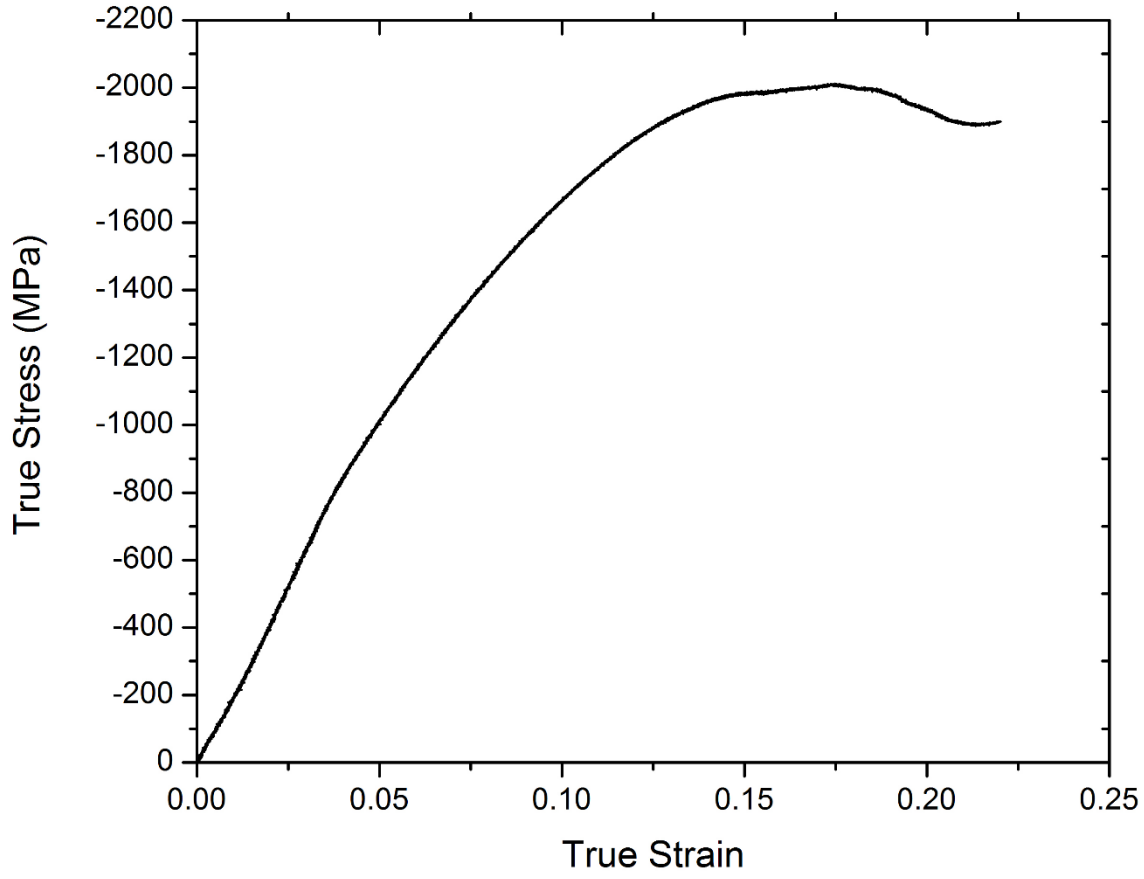

Fig. 28 Compressive true stress-strain curve of sintered sample

CHAPTER 6 CONCLUSIONS

Low density steels are exciting replacement of convectional steels mainly in automobile industry. Its main advantage of high specific weight to strength ratio is cause of attraction of these steels in automobile industry. The non-equilibrium processing route of steels has shown some exciting properties which are better when compared with equilibrium processed steels. The bulk formed from mechanical alloyed Fe-Al-Mn-C powder using spark plasma sintering has exotic microstructure and excellent mechanical properties. Process parameters optimization for maximum consolidation was first and main step in this work. Once desired consolidation had been achieved then mechanical testing was done which had given attracting results. The hardness of steel comes out to be 920VHN which is quite high when compared with 500VHN of melted steel. This was because of fine grains due to non-equilibrium processing of steel. The compressive strength of steel comes out to be 2.08GPA which is excellent for its application under compressive loading in automobile industry. The proof strength of 1.6GPA was obtained which is impressive. The future work will be to make a bulk with maximum densification for tensile text. If material give better tensile properties as expected then its attractiveness in automobile industry will increase further.

CHAPTER 6 REFERENCES

[1] R. Rana, C. Lahaye, and R. K. Ray, "Overview of Lightweight Ferrous Materials: Strategies and Promises," *Jom*, vol. 66, no. 9, pp. 1734–1746, (2014).

[2] R. Rana, C. Liu, and R.K. Ray, Scr. Mater. 68, 354 (2013)

[3] R. Rana and C. Liu, Philos. Mag. Lett. 93, 502 (2013).

[4] K.T. Park, Scr. Mater. 68, 375 (2013).

[5] Y.G. Kim, J.M. Han, and J.S. Lee, Mater. Sci. Eng. A 114, 51 (1989).

[6] S.W. Hwang, J.H. Ji, E.G. Lee, and K.-T. Park, Mater. Sci. Eng. A 528, 5196 (2011).

[7] T. Sahraoui, M. Hadji, and M. Yahi, Mater. Sci. Eng. A 523, 271 (2009).

[8] R. Rana, C. Liu, and R.K. Ray, Scr. Mater. 68, 354 (2013).

[9] C. Liu and R. Rana, European patent application no. EP12163765.6, 2011.

[10] R.K. You, P.-W. Kao, and D. Gan, Mater. Sci. Eng. A 117, 141 (1989).

[11] S.S. Sohn, B.-J. Lee, S. Lee, N.J. Kim, and J.-H. Kwak, Acta Mater. 61, 5050 (2013).

[12] G. Frommeyer, E.J. Drewes, and B. Engl, La Rev. Me´tall. 97, 1245 (2000).

[13] G. Frommeyer and U. Bru ¨x, Steel Res. Int. 77, 627 (2006).

[14] J.D. Yoo and K.-T. Park, Mater. Sci. Eng. A 496, 417 (2008).

[15] U. Brux, G. Frommeyer, and J. Jimenez, Steel Res. Int. 73, 543 (2002).

[16] R. Rana and C. Liu, Can. Metall. Q. 53, 300 (2014).

[17] I. Zuazo, Y. Brechet, and P. Maugis, New Developments on Metallurgy and Applications of High Strength Steels (Warrendale, PA: TMS, 2008), pp. 1245–1253.

[18] G.B. Olson and M. Cohen, Metall. Trans. A 7, 1897 (1976).

[19] G.B. Olson and M. Cohen, Metall. Trans. A 7, 1905 (1976).

[20] W.S. Yang, K.H. Hwang, T.B. Wu, J.G. Byrne, and C.M. Wan, Scr. Metall. Mater. 24, 1221 (1990).

[21] S.L. Case and K.R. Van Horn, Aluminum in Iron and Steel (New York: Wiley, p. 4, (2004)

[22] R.A. Hadfield, U.S. patent 422,403 (1897).

[23] R.A. Hadfield, Trans. Am. Inst. Min. Eng. 19, 1041 (1891).

[24] R. Oshima and C.M. Wayman, Metall. Trans. 3, 2163 (1972).

[25] L.S. Palatnik, I.A. Tananko, and Y.G. Bobro, Sov. Phys. Crystallogr. 9, 163 (1964).

[26] A. Inoue, T. Minemura, A. Kitamura, and T. Masumoto, Metall. Trans. A 12A, 1041 (1981).

[27] K.H. Hwang, C.M. Wan, and J.G. Byrne, Mater. Sci. Eng. A 132, 161 (1991).

[28] G. Frommeyer, E.J. Drewes, and B. Engl, Rev. Metall. 10, 1245 (2000).

[29] C. J. Altstetter, A. P. Bentley, J. W. Fourie, and A. N. Kirkbride, "Processing and properties of FeMnAl alloys," Mater. Sci. Eng., vol. 82, no. C, pp. 13–25, (1986).

[30] R. Rana, C. Lahaye, and R. K. Ray, "Overview of Lightweight Ferrous Materials: Strategies and Promises," *Jom*, vol. 66, no. 9, pp. 1734–1746, (2014).

[31] Y. Minamino, Y. Koizumi, N. Tsuji, N. Hirohata, K. Mizuuchi, and Y. Ohkanda, "Microstructures and mechanical properties of bulk nanocrystalline Fe-Al-C alloys made by mechanically alloying with subsequent spark plasma sintering," *Sci. Technol. Adv. Mater.*, vol. 5, no. 1–2, pp. 133–143, (2004).